

$^{84}\text{Kr}$ -induced reactions where the centroid in  $Z$  is shifted to larger values corresponding to net transfer of mass from the target to the projectile.<sup>3</sup> Based on potential energies of the two-nucleus intermediate systems, the driving force for mass transfer to the projectile is much greater for the reaction  $^{209}\text{Bi} + ^{84}\text{Kr}$  than for the reaction  $^{209}\text{Bi} + ^{136}\text{Xe}$ .

In summary, the charge distributions are interpreted in terms of a strong contact collision between the two complex nuclei resulting in a two-body intermediate system where the two nuclei cling together temporarily but do *not* actually fuse together. The reaction products "remember" to some extent their initial charges and masses as well as their direction of motion. During the time of contact of the two nuclear surfaces, translational energy is converted into internal energy and nucleon transfer occurs between the fragments. Accordingly, the broader  $Z$  distributions correspond to longer interaction times and larger kinetic-energy losses.

†Work performed under the auspices of the U. S. Energy Research and Development Administration.

\*Work supported in part by the German Bundesministerium für Bildung und Wissenschaft.

<sup>1</sup>A. G. Artukh, G. F. Gridnev, V. L. Mikheev, V. V. Volkov, and J. Wilczyński, Nucl. Phys. **A215**, 91 (1973).

<sup>2</sup>F. Hanappe, M. Lefort, C. Ngô, J. Péter, and B. Ta-

main, Phys. Rev. Lett. **32**, 738 (1974).

<sup>3</sup>K. L. Wolf, J. P. Unik, J. R. Huizenga, J. R. Birkelund, H. Freiesleben, and V. E. Viola, Phys. Rev. Lett. **33**, 1105 (1974).

<sup>4</sup>S. G. Thompson, L. G. Moretto, R. C. Jared, R. P. Babinet, J. Galin, M. M. Fowler, R. C. Gatti, and J. B. Hunter, Phys. Scr. **10A**, 36 (1974).

<sup>5</sup>J. Péter, C. Ngô, and B. Tamain, J. Phys. (Paris), Lett. **36**, L23 (1975).

<sup>6</sup>J. C. Jacmart, P. Colombani, H. Doubre, N. Frascaria, N. Poffé, M. Riou, J. C. Roynette, C. Stéphan, and A. Weidinger, Nucl. Phys. **A242**, 175 (1975).

<sup>7</sup>P. Colombani, N. Frascaria, J. C. Jacmart, M. Riou, C. Stéphan, H. Doubre, N. Poffé, and J. C. Roynette, Phys. Lett. **55B**, 45 (1975).

<sup>8</sup>J. Wilczyński, K. Siwek-Wilczyńska, J. S. Larsen, J. C. Acquadro, and P. R. Christensen, Nucl. Phys. **A244**, 147 (1975).

<sup>9</sup>R. Albrecht, W. Dünneberger, G. Graw, H. Ho, S. G. Stadman, and J. P. Wurm, Phys. Rev. Lett. **34**, 1400 (1975).

<sup>10</sup>R. Vandenbosch, M. P. Webb, and T. D. Thomas, to be published.

<sup>11</sup>T. M. Cormier, A. J. Lazzarini, M. A. Neuhausen, A. Sperduto, K. Van Bibber, F. Videbaek, G. Young, E. B. Blum, L. Herreid, and W. Thoms, to be published.

<sup>12</sup>R. Babinet, L. G. Moretto, J. Galin, R. Jared, J. Moulton, and S. G. Thompson, to be published.

<sup>13</sup>J. R. Birkelund, J. R. Huizenga, H. Freiesleben, K. L. Wolf, J. P. Unik, and V. E. Viola, Jr., Phys. Rev. C (to be published).

<sup>14</sup>L. C. Northcliffe and R. F. Schilling, Nucl. Data, Sect. A **7**, 233 (1970).

## Magnetic Splitting of Quasimolecular Electronic States in Strong Fields\*

Johann Rafelski and Berndt Müller

Argonne National Laboratory, Argonne, Illinois 60439

(Received 28 October 1975)

The heavy-ion motion in sub-Coulomb collisions generates extreme magnetic fields. The hyperfine splitting of the spin- $\frac{1}{2}$  quasimolecular electronic states in  $U+U$  is found to reach 10% of the molecular binding energy (100 keV). Also  $Pb+Pb$  and  $Xe+Xe$  collisions are considered.

In order to test the behavior of matter in very strong magnetic fields, an experiment has to fulfill two conditions: (1) Extremely high currents are needed as the source of the magnetic field, and (2) the probing charge must be in the close vicinity of the current because of the dipole character of the magnetic field. In sub-Coulomb-barrier heavy-ion collisions the magnetic field created in the vicinity of the colliding nuclei is of the order of  $10^{14}$  G, however over a rather small volume. (In a constant magnetic field of this size

the Zeeman splitting of the spin states of an electron would be comparable to its rest mass.) For our considerations it is important to recognize that the inner-shell electrons move in the force field generated by the colliding heavy ions: These electrons are bound by both nuclei and form quasimolecular states.<sup>1,2</sup> Under certain conditions to be discussed below, this leads to the localization of the inner-shell electronic wave functions in the region of strong magnetic fields.

In the quasimolecule the main binding is provid-

ed by the electrostatic potential of the two nuclei, while the magnetic "hyperfine" splitting of the electronic states may reach  $0.2m$  in selected systems. This is the case because the effective electric coupling constant is  $Ze^2$ , whereas it is  $Ze^2v/c$  for the magnetic interaction. The spinor wave functions of relativistic electrons in the collision system are found by solving the two-center Dirac equation<sup>3</sup> ( $\hbar=c=1$ ),

$$\left(\vec{\alpha} \cdot \vec{p} + \beta m - \frac{Z_1 e^2}{|\vec{r} - \vec{R}/2|} - \frac{Z_2 e^2}{|\vec{r} + \vec{R}/2|}\right)\psi = E\psi, \quad (1)$$

where  $\vec{\alpha}$  and  $\beta$  are the Dirac matrices and  $R$  is the internuclear distance. (The electron-electron interactions are neglected here; we will discuss their effects below.)  $E$  is the total energy of the electron and is related to the binding energy  $E_B$  by  $E = m - E_B$ . The energy spectrum of Eq. (1) consists of discrete bound states in the interval  $-m < E < +m$ , electron scattering states for  $E > m$ , and positron scattering states for  $E < -m$ . In the case that  $Z_1 + Z_2 > 137$  and for separations  $R < R_{cr}$ , electronic bound states can exist as resonance states in the negative-energy continuum.<sup>4</sup>  $R_{cr}$  is the critical distance between the nuclei at which the binding energy of the most strongly bound electrons exceeds  $2m$ .

The vector potential  $\vec{A}$  present in the heavy-ion collision (as seen from the c.m. system) is obtained from

$$e\vec{A} = -Ze^2 \frac{\vec{V}_1}{|\vec{r} - \vec{R}/2|} - Ze^2 \frac{\vec{V}_2}{|\vec{r} + \vec{R}/2|}. \quad (2)$$

(We have restricted our calculations to symmetric collisions and  $\vec{V}_i$  are the heavy-ion velocities.) It is important to realize that the corresponding magnetic field cannot be transformed away by a choice of a suitable inertial frame.

The heavy-ion velocity can be divided into a radial part  $v_\rho$  and an angular one  $v_\varphi$  (the  $z$  direction is along the internuclear axis):

$$v_\rho = \frac{1}{2}v_\infty(1 - 2Z^2e^2/RE_{kin} - b^2/R^2)^{1/2}, \quad (3a)$$

$$v_\varphi = bv_\infty/2R. \quad (3b)$$

Here  $E_{kin}$  and  $v_\infty$  are the (lab system) projectile kinetic energy and velocity before the collision, and  $b$  is the impact parameter.

The magnetic interaction Hamiltonian of the relativistic electrons bound to the molecular sys-

tem is given by ( $\alpha_\rho$  and  $\alpha_\varphi$  are Dirac matrices)

$$\begin{aligned} H_{mag} &= H_\rho + H_\varphi \\ &= -Ze^2(v_\rho\alpha_\rho + v_\varphi\alpha_\varphi) \\ &\quad \times (|\vec{r} - \vec{R}/2\rangle^{-1} - |\vec{r} + \vec{R}/2\rangle^{-1}). \end{aligned} \quad (4)$$

In the basis of Eq. (1) the magnetic states of opposite spin are degenerate. Therefore, the calculation of the magnetic splitting due to  $H_{mag}$  proceeds via degenerate-state perturbation theory.

It should be noted that only the  $\alpha_\rho$  part of the interaction (4) contributes to the diagonal elements in the secular matrix if  $\alpha_\rho$  is chosen to be  $\gamma_5\sigma_z$ , while the off-diagonal elements are then matrix elements of  $H_\varphi$ . In the simplest case of spin- $\frac{1}{2}$  states ( $1s\sigma$  and  $2p_{1/2}\sigma$ ) the energy change of the spin-up and spin-down states is

$$E_{\uparrow} - E_{\downarrow} = \mp (|\langle \uparrow | H_\rho | \uparrow \rangle|^2 + |\langle \uparrow | H_\varphi | \uparrow \rangle|^2)^{1/2}. \quad (5)$$

It is evident from the definition of  $H_{mag}$  [Eq. (4)] that the dynamical parameters  $E_{kin}$  and  $b$  of a particular collision enter only via  $v_\rho$  and  $v_\varphi$ . Let us therefore introduce the matrix elements

$$\mathfrak{M}_\varphi = \langle \uparrow | -Ze^2\alpha_\varphi(|\vec{r} - \vec{R}/2\rangle^{-1} - |\vec{r} + \vec{R}/2\rangle^{-1}) | \uparrow \rangle, \quad (6a)$$

$$\mathfrak{M}_\rho = \langle \uparrow | -Ze^2\alpha_\rho(|\vec{r} - \vec{R}/2\rangle^{-1} - |\vec{r} + \vec{R}/2\rangle^{-1}) | \uparrow \rangle, \quad (6b)$$

which depend only on  $Z$  and the nuclear separation  $R$ .

To evaluate these matrix elements we have to solve Eq. (1), which, in contrast to its nonrelativistic counterpart, is not separable in two coordinates. We have used an approach in which one variable is made discrete by the expansion of the Dirac wave function in spinor multipoles. The two-dimensional equation reduces then to an infinite system of coupled first-order differential equations. This system was truncated at a sufficiently large angular momentum  $j_{max}$ . The resulting system of  $2(2j_{max} + 1)$  coupled differential equations was solved iteratively for the energy eigenvalue and  $2j_{max}$  coefficients describing the behavior of the wave function at the origin. In order to obtain good wave functions we required convergence of the  $2j_{max} + 1$  eigenvalues to better than  $10^{-10}$ . However, because of the truncation of the Hilbert space, the true eigenvalue was only established to a relative precision of 0.1%. The direction of the iteration was determined by the use of the  $(2j_{max} + 1)$ -dimensional steepest-de-

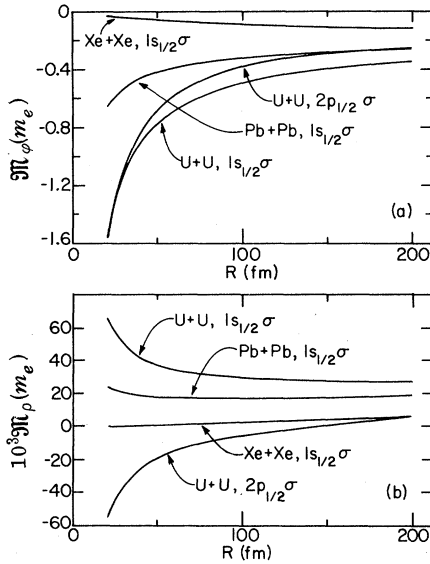


FIG. 1. The magnetic-coupling matrix elements  $\mathfrak{M}$ : (a) the rotational  $\mathfrak{M}_\phi$  and (b) the radial magnetic coupling  $\mathfrak{M}_\rho$ , as a function of internuclear distance  $R$ , for Xe+Xe, Pb+Pb, U+U  $1s\sigma$ , and U+U  $2p_{1/2}\sigma$  electronic quasimolecular states.

scent method. We have tested the accuracy of our program by comparison of the united-atom-limit solutions with the analytic solutions of the spherical Dirac equation. Furthermore we have compared our calculations of molecular energies with the results obtained from a diagonalization procedure developed before.<sup>3</sup> The eigenstates embedded in the continuum were calculated by actual integration of the Dirac equation for  $E < -m$ . The oscillating part of the wave function at large distances was truncated.

We have used these wave functions to calculate the matrix elements defined in Eq. (6), which are shown in Figs. 1(a) and 1(b) as a function of  $R$  for the systems U+U ( $1s_{1/2}\sigma$  and  $2p_{1/2}\sigma$ ), Pb+Pb ( $1s_{1/2}\sigma$ ), and Xe+Xe ( $1s_{1/2}\sigma$ ). In the region  $20 \text{ fm} < R < 200 \text{ fm}$  the velocity components  $v_\phi$  and  $v_\rho$  are comparable (except for the unlikely case of backward collisions). Therefore the rotational magnetic coupling is dominant,  $\mathfrak{M}_\phi$  being 30 times larger than  $\mathfrak{M}_\rho$ .

In the united-atom limit we can evaluate the  $\mathfrak{M}_\phi$  matrix element between nonrelativistic Pauli spinors analytically and we find good agreement with our calculations in the Xe+Xe system. We also find that the matrix element scales as the fourth power of  $Z$ . The relativistic corrections enhance the dependence on  $Z$  due to the partial collapse of the wave function to the center<sup>5</sup> which brings the electrons to the region of strong mag-

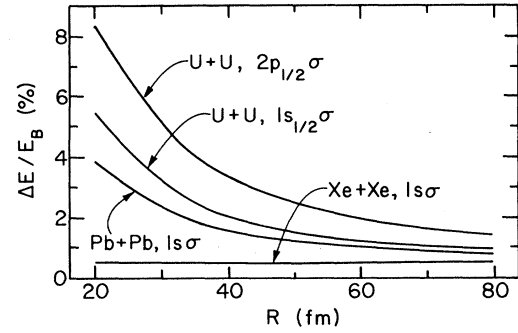


FIG. 2. The relative magnetic splitting  $(E_+ - E_-)/E_B$  for the four discussed quasimolecular states. Collision parameters are  $E_{\text{kin}}/N = 9 \text{ MeV/nucleon}$  and  $b = 13 \text{ fm}$ .

netic field strength.

We have calculated the magnitude of the splitting  $\Delta E$  of the opposite spin states following from Eq. (5) using the collision parameters  $b = 13 \text{ fm}$  and  $E_{\text{kin}}/N = 9 \text{ MeV/nucleon}$ . The relative splittings  $\Delta E/E_B$  are shown in Fig. 2 as a function of  $R$  for the above-mentioned scattering systems. We find that the relative magnetic splitting of the  $2p_{1/2}\sigma$  level in U+U is very large and exceeds that of the  $1s\sigma$  state because the binding energy is considerably smaller, while the matrix elements are of the same size. The energies of the U+U molecular states in discussion are shown in Figs. 3(a) and 3(b). The relative splitting of the  $1s\sigma$  state in Xe+Xe may be too small to be detectable.

In view of these results we feel that any experiment to test the behavior of electrons in the

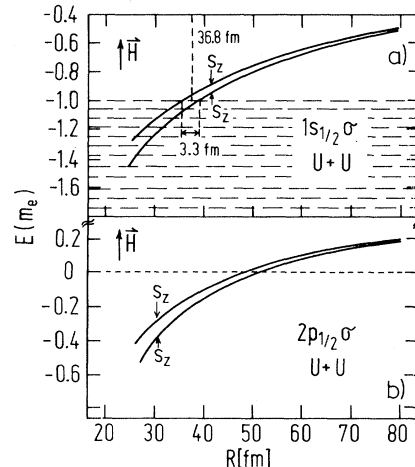


FIG. 3. The four quasimolecular states with magnetic interaction which are discussed in the text. Collision parameters are  $E_{\text{kin}}/N = 9 \text{ MeV/nucleon}$  and  $b = 20 \text{ fm}$ . (a) U+U,  $1s_{1/2}\sigma$  (the spin-parallel state reaches the negative-energy continuum 3.3 fm earlier than the state with antiparallel spin). (b) U+U,  $2p_{1/2}\sigma$ .

strong magnetic field should possibly be carried out in a system as heavy as Pb+Pb. As the system becomes heavier an investigation of the splitting of the  $2p_{1/2}\sigma$  level seems to be advantageous, since it is much easier to have this state ionized in the collision.

The U+U molecular levels were calculated without the inclusion of electron screening and virtual vacuum polarization. Also, the finite size of the U nuclei has been neglected.<sup>3</sup> Those effects combined would shift the energies by approximately 100 keV upwards, parallel to the plotted curves in Fig. 3. We estimate the shift in  $R_{cr}$  due to the neglected effects to be 3 fm. The magnetic interaction causes the spin-up state to join the negative continuum 3.3 fm earlier than the spin-down state. The true critical radius lies at 36 fm for the spin-up state in the U+U system including the above-mentioned corrections. Our calculations are in good agreement with the previous results from the diagonalization of the Dirac equation.<sup>3</sup> The approximate variational calculations by Marinov and Popov<sup>6</sup> give significantly larger  $R_{cr}$  (51 fm).

We have investigated the various dynamic couplings within the two-state system and found that the rearrangement of vacancies between the spin states is negligible. Therefore, the distribution of vacancies in the magnetic substates of the K shell after the heavy-ion collision is determined by the dynamical coupling of the substates to higher electronic states. This causes the polarization degree of the subsequent  $K\alpha$  radiation to be sensitive to the ionization mechanism for the molecular states. If the ionization occurs in the region of strong magnetic splitting ( $R \lesssim 200$  fm) then the ratio between the two photon polarization states after the collision will be  $\sigma_{\downarrow}/\sigma_{\uparrow} \approx e^{+\Delta E/\Gamma} \sim 1 + \Delta E/\Gamma > 1$ .  $\Gamma$  is the dynamic collision broadening of the molecular  $1s\sigma$  state, and we estimate  $\Delta E/\Gamma \sim 0.2$ . On the other hand, if ionization occurs in the periphery of the collision then the two spin states will be differently refilled and  $\sigma_{\downarrow}/\sigma_{\uparrow} \lesssim 1$ . Here the deviation from unity should be much smaller than in the first case: The density of vacancies is much lower in the inner shell.

The size of the magnetic field is best demonstrated by the ratio of the equivalent magnetic moment generated in the heavy-ion collision to the proton magnetic moment:

$$\mu_{HI} = Zevb \sim 6 \times 10^{-17} Z \text{ MeV/G} \sim 20Z\mu_p. \quad (7)$$

Therefore the magnetic field is considerably larger than the fields in the vicinity of nuclei that can be tested in hyperfine-structure experiments. Certainly the precision of those experiments is significantly larger; nonetheless the experiment we propose opens a new regime of magnetic fields to laboratory tests, which is especially important if higher-order effects in magnetic fields are present.

Laboratory magnetic fields, although smaller by many orders of magnitude, can be increased by accelerator experiments by a factor  $\gamma = E/m$  as a result of the Lorentz transformation.<sup>7</sup> Present day accelerators allow  $\gamma \sim 2 \times 10^4$  while the magnetic field strength attainable is  $B \sim 5 \times 10^6$  G, giving an equivalent field of  $10^{11}$  G, compared to an average  $10^{14}$  G in a heavy-ion experiment.

---

\*Work performed under the auspices of the United States Energy Research and Development Administration.

<sup>1</sup>Experimental confirmation of this fact in heavy-ion-atom collisions with  $Z_1 + Z_2 > 70$  was established by P. H. Mokler, H. J. Stein, and P. Armbruster, *Phys. Rev. Lett.* **29**, 827 (1972); W. E. Meyerhof, T. K. Saylor, S. M. Lazarus, W. A. Little, and B. B. Triplett, *Phys. Rev. Lett.* **30**, 1279 (1973); D. Burch, W. G. Ingalls, H. Wieman, and R. Vandenbosch, in *Proceedings of the Ninth International Conference on the Physics of Electronic and Atomic Collisions, Seattle, July 1975* edited by J. S. Risley and R. Geballe (Univ. of Washington Press, Seattle, Wash., 1975), p. 306; P. Gippner, K. H. Kaun, F. Stary, W. Schulze, and Yu. P. Tretjakov, *Nucl. Phys. A230*, 509 (1974).

<sup>2</sup>A discussion of the adiabaticity conditions in super-heavy quasimolecules can be found in J. Rafelski, B. Müller, and W. Greiner, *Lett. Nuovo Cimento* **4**, 469 (1972).

<sup>3</sup>B. Müller, J. Rafelski, and W. Greiner, *Phys. Lett.* **47B**, 5 (1973); B. Müller and W. Greiner, to be published.

<sup>4</sup>B. Müller, H. Peitz, J. Rafelski, and W. Greiner, *Phys. Rev. Lett.* **28**, 1235 (1972); Ya. B. Zel'dovich and V. S. Popov, *Usp. Fiz. Nauk* **105**, 403 (1971) [*Sov. Phys. Usp.* **14**, 673 (1972)].

<sup>5</sup>W. Pieper and W. Greiner, *Z. Phys.* **218**, 327 (1969).

<sup>6</sup>M. S. Marinov and V. S. Popov, *Zh. Eksp. Teor. Fiz.* **68**, 421 (1975) [*Sov. Phys. JETP* **41**, 205 (1975)]; M. S. Marinov, V. S. Popov, V. L. Stolin, *Pis'ma Zh. Eksp. Teor. Fiz.* **19**, 76 (1973) [*JETP Lett.* **19**, 49 (1974)].

<sup>7</sup>T. Erber, *Rev. Mod. Phys.* **38**, 626 (1966).